sciendo

DOI: 10.2478/ata-2023-0001



Acta Technologica Agriculturae 1
Nitra, Slovaca Universitas Agriculturae Nitriae, 2023, pp. 1–8

# MODELLING OF IMPULSE FUNCTIONS OF ULTRASONIC SENSORS WHEN TILT ANGLE OF REFLECTING SURFACE IS CHANGED

Vladimír MADOLA[1], Vladimír CVIKLOVIČ*[1], Krzysztof ROKOSZ[2]

[1]Slovak University of Agriculture in Nitra, Faculty of Engineering, Institute of Electrical Engineering, Automation, Informatics and Physics, Nitra, Slovakia; xmadolav@uniag.sk (V.M.)
[2]Koszalin University of Technology, Faculty of Electronics and Computer Science, Department of Computer Science and Management, Koszalin, Poland; krzysztof.rokosz@tu.koszalin.pl

*correspondence: vladimir.cviklovic@uniag.sk

Increasing the accuracy of position measurement is an intensively addressed issue in engineering practice. Indirect methods provide satisfactory distance information. For more accurate identification of surface geometry or tilt, systems based on image processing are frequently employed, however, these are more expensive in contrast to devices operating on the basis of acoustic principle. This paper deals with the modelling of the impulse functions of ultrasonic sensors under known geometrical conditions of their distribution. The reflecting surface is a metallic surface. Based on the results, a statistically significant non-linear correlation between the complex integral of the impulse function and the front time of the transient characteristic is shown. The change from the parallel to the perpendicular case of the longitudinal axis of ultrasonic transducer distribution due to the change in the tilt angle of reflected surface is also included in the study. The interval of change in the tilt angle of reflecting surface was from 0° to 30°.

**Keywords:** impulse function; ultrasound echo; ultrasound reflection; Hilbert transformation; measurement of angle; ultrasound

A common method for measuring the distance is with a calibrated mechanical device that simultaneously connects the selected point, the distance of which is being measured to a reference position. The main disadvantages of contact measurement include time-consuming nature and limitation in terms of the maximum distance. As the required measurement range increases, measurement uncertainty increases, and thus it is advantageous to use a non-contact distance measurement method. Non-contact distance measurement is based on energy postulate and is divided into active method – energy emission correlated with the known rate of energy propagation in the environment, and passive method – detection of the natural emission of an energy form from an object in the environment correlated with the known rate of energy propagation in the environment (Webster and Eren, 2014; Lu, 2014). The acoustic form of energy provides an inexpensive method of non-contact distance measurement. The frequencies of acoustic waves above the audible spectrum (typically 40 kHz and higher) are used for measurement. Ultrasonic transducers are lightweight and inexpensive devices, which are typically implemented based on the piezoelectric principle. The advantage is immunity to electromagnetic interference (Ishikara et al., 2009). Their disadvantage lies in their inferior directional characteristics in contrast to optical sensors (Yata et al., 2000). Hrubý et al. (2022) implemented the VL53L1X optical distance sensor in the experimental range up to 4000 mm under light conditions of 10 lx and 350 lx, obtaining the highest root mean square error of measurements for the colour variation of reflecting surface to black at a value of 10.10 mm, at a distance of 2000 mm. Moreover, they modelled the measurement error waveform by linear regression at a root mean square measurement error in the interval 3.10 mm ÷ 10.10 mm. Echolocation refers to the process of measuring position by determining the time it takes for an echo to return from the object to the measuring device. If the reflected impulse is measured simultaneously by multiple sensors, the direction of the object can also be measured (Lim and Leonard, 2000). Rabadan et al. (2017) experimentally observed that the maximum relative error of the distance measured by the ultrasonic pulse with a frequency of 40 kHz with respect to the optical distance measurement took a value of -2.00% error for a real length of 800 mm. The amplitude of reflected ultrasonic waves together with the time of their detection from the reflected object can be used to detect wall-corner surfaces. For the purposes of the amplitude-only model, the reflection coefficient of the surfaces in question must be considered (Martínez et al., 2004). Using the impulse response of the ultrasonic transducer, the received acoustic signal can be analysed in the time plane using a Dirac impulse. The shape factor of the received impulse can be used to detect straight reflection planes or sharp corners and edges. However, it is necessary to use the convolution operator. A Gaussian harmonic envelope can also be used to approximate the shape of the acoustic impulse that is received by the ultrasonic transducer. One can partially decompose the image area into differentials and investigate the impulse responses in geometrical view with the help of Huygens's principle (Kuc and Siegel, 1987). The ultrasound signal processing by computation of the envelope waveform is possible by Hilbert transform or by the absolute difference of the ultrasound signal from the noise at the sensor. The discrete Fourier transform can be

used to determine the dominant frequency component of the acquired signal (Shin et al., 2019). Moreira et al. (2020) stated that an unfiltered envelope of the ultrasound signal can obtain an error of 4.78% in the on-plane position of an object at a measurement distance of 845 mm by using two sensors. The use of the ultrasound signal envelope is intended for a more exact definition of the instant of acoustic impulse sensing by the ultrasonic transducer. It is necessary to perform a Hilbert transform of the acoustic signal and a summation in the complex plane with the time history of the acoustic signal, which is demanding on the hardware on which the measurement system is implemented (Xu et al., 2009). The identification of linear dynamic systems is treated as a response to an impulse function. The time integral and the steady-state value of the transient characteristic can provide significant differences in the quantization index under geometrical conditions. A non-linear correlation between the amplitude of the ultrasound signal and the distance between transmitter and transducer is assumed. The paper presented deals with the statistical evaluation of acoustic signal amplitudes as a function of the distance between the ultrasound source and the ultrasonic sensors. The spatial distribution of ultrasonic sensors in space under angular vector variation was proposed. The frequency of acoustic waves was 40 kHz. It is useful to determine the type of reflecting surface especially in case of mobile robotics, such as tracking a perpendicular surface when guiding the robot or creating a space map when considering planes. Ureña et al. (1999) presented the determination of the inclined plane by the method of known reflection surface distances determined by ultrasonic sensors. A minimum of two ultrasonic transducers must be used.

## Material and methods

### Measuring system

A measurement system protected by a patent (Lendelová et al., 2017) was used as a source of acoustic waves. The distance measurement was performed by the impulse method of position vector measurement. The microcontroller included in the used measurement system allows control of the length of the transmitted acoustic wave via frequency output. A block diagram of the measurement system is shown in Fig. 1.

The MOSFET bridge TC4428 by Microchip Technology Inc. was employed as a power amplifier for ultrasonic transmission. For measurement purposes, the supply voltage at output played particularly important role, with a typical value of 18 volts, and the switching period of the power output converted to a maximum frequency of 16.6 MHz (Microchip Technology, 2014). The ultrasonic transmitter with a DC voltage of 12 volts was switched symmetrically at a switching frequency of 1 Hz. The microcontroller used was an 8-bit architecture from SiLabs, analogue-intensive class C8051F410. The data source was represented by an analogue-to-digital converter, which was located directly on the microcontroller. For recording of measured data, an Agilent U2353A data logger (Keysight, 2021) was utilized (Table 1). The software Agilent Measurement Manager 1.2 was utilized for the purposes of interface.

The microcontroller firmware development was carried using a Keil µVision 5.25 licenced integrated development environment in conjunction with the Silabs 8-bit USB Debug

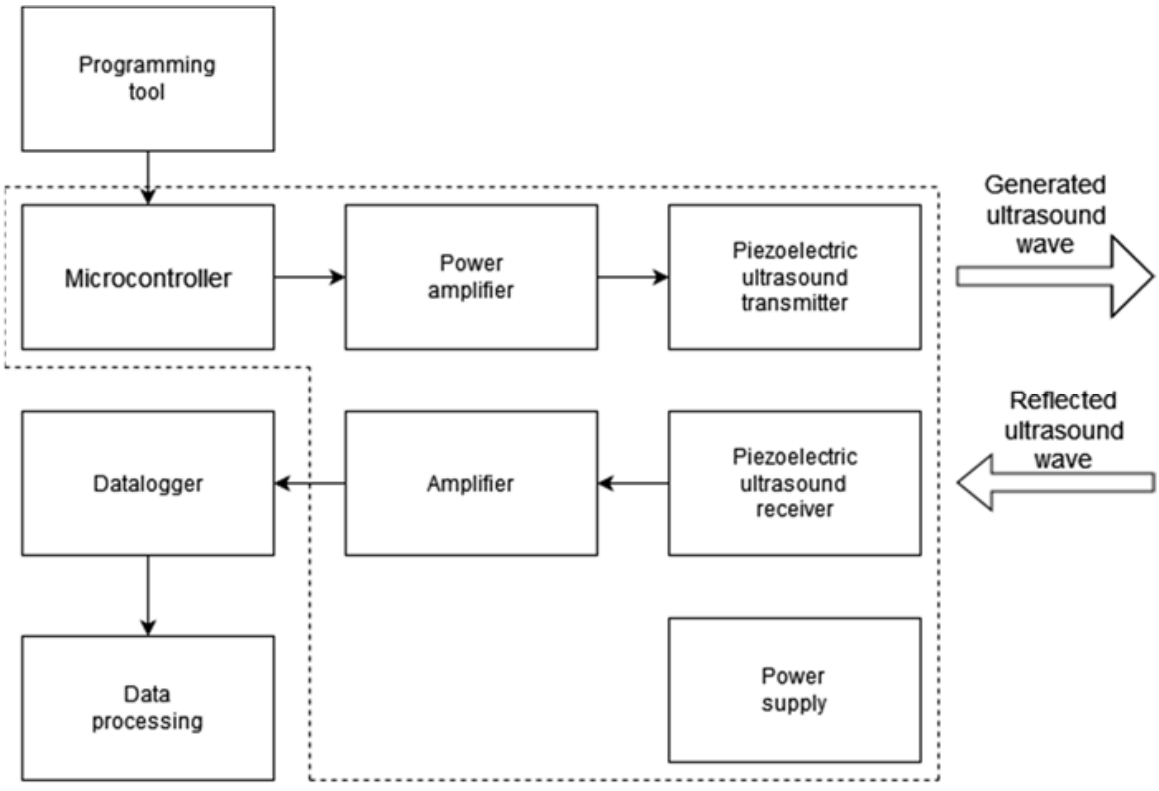



**Fig. 1** Block diagram of the measuring system

Adapter. The amplification of received acoustic signal was realized by cascading two TL074CN operational amplifiers in an inverting circuit with an absolute gain of 25.334 dB. The input impedance was set to 1 kΩ.

**Table 1** Selected characteristics related to Agilent U2353A device

| Parameter | Value (unit) |
|---|---|
| **Number of analogue channels** | 16 (-) |
| **Resolution** | 16 (bit) |
| **Maximum sampling rate** | 1 (MSa·s$^{-1}$) |
| **Bipolar input range** | ±10; ±5; ±2.5; ±1.25 (V) |
| **Input impedance** | 1 (GΩ) / 100 (pF) |
| **Offset error** | 1 (mV) |
| **Slew rate** | 19 (V·µs$^{-1}$) |
| **Accuracy** | 0.02 ÷ 0.12 (%) + 1.0 (mV) |

Source: Keysight, 2021

### Piezoelectric ultrasonic sensor

A Pro-Wave Electronic Corp. 400ST/R160 piezoelectric acoustic transducer of open circular design was used in an assembly of one transmitter and five receivers. The transducer resonant frequency was (40.0 ±1.0) kHz. The angular direction vector was specified to be ±27.5° in condition -6 dB related to standard attenuation criteria (Pro-Wawe, 2005).

### Analysis of acoustic signal

The amplitude model (Eq. 1), based on the research conducted by Martínez et al. (2003) and adapted to the plane reflection case, can be applied to non-linear regression of immediate amplitude values, depending on the angle of 'ultrasonic sensor's view':

$$U = U_{\max} \times C \frac{e^{(-2kx)}}{2x} \times e^{\left(-\frac{4\varphi^2}{\varphi_0^2}\right)} \quad (1)$$

where: $U$ – amplitude of measured voltage on ultrasonic sensor (V); $U_{\max}$ – constant, independent on the type of reflecting surfaces or material of reflecting surfaces (V); $C$ – correction factor of voltage in specific case (known distance between transducer and reflected plane); $k$ – coefficient of attenuation (dB·m$^{-1}$); $x$ – distance between the ultrasonic transmitter and reflecting surface (m); φ – detection angle under which target is viewed by the sensor (°); $\varphi_0$ – minimal angle of ultrasound waves detects by the sensor (°)

The measured data were modelled using a transfer function (Eq. 2) (Smith, 1999). The criterion of highest fit with the experimental data was used.

$$G(s) = \frac{Y(s)}{X(s)} \quad (2)$$

where: $G(s)$ – transfer function of complex variable; $Y(s)$ – output vector of linear dynamic system; $X(s)$ – input vector of linear dynamic system

By time-integrating, the obtained transfer function (Eq. 2) via iteration method and plotting the steady-state criterion of the output vector in the set of the real variable, one obtains:

$$y(\infty) \rightarrow L^{-1}\left[\frac{1}{s}G(s)\right] \quad (3)$$

where: $y(\infty)$ – the steady-state value of the impulse response time function; $L^{-1}$ – inverse Laplace transform operator

The criterion for determining the order of transfer function of a dynamic system is the correlation coefficient $R_x$ (Fikar and Mikleš, 1999), to which Eq. 4 is related. For the tightness criterion, the correlation coefficient $R_x$ is guided to be maximized to the highest extent. For the coefficient of determination $R^2$, the analogy can be expressed as follows:

$$R_x = \sqrt{(\Delta t_s)^{-1} \times \int_{\Delta t_s} \varepsilon^2(t)dt} \quad (4)$$

$$R^2 = R_x^2 \times 100 \quad (5)$$

where: $R_x$ – the coefficient of correlation of transfer function to measured data; $t$ – time (s); $\Delta t_s$ – time differential (independent variable) of the transfer function dataset (s); $\epsilon$ – deviation between identified point of transfer function and corresponding real measured data point; $R^2$ – the coefficient of determination (goodness of fit) of transfer function to measured data (%)

By approximating the impulse function, the ultrasonic impulse can be modelled for specific conditions. However, Kuc and Siegel (1987) took into consideration the Huygens principle of partial reflections in their work, which does not represent the expression generality. The impulse time waveform on the ultrasonic sensor can be quantified by an envelope function (Eq. 6). The use of an ultrasound signal envelope is useful precisely in determining the time difference of the ultrasound reflection capture or in analysing the ultrasound signal by convolution (Pare at al., 2020). The Hilbert transform in the general form $jh(y)$ according to Euler was used to obtain the envelope function ye of the sensor impulse function $y(t)$:

$$y_e = \sqrt{y(t) + jh(y)} \quad (6)$$

### Measurement conditions

A metal surface with dimensions of 245 mm × 220 mm × 1 mm was exposed to ultrasonic waves. The distance between the ultrasonic transmitter and the reflection surface was 190 mm by a conical approach according to Eq. 7 in the straight case. The experimental conditions are shown graphically in Fig. 2. The distance between the ultrasonic transducer and reflected surface was 190 mm. The variation of inclination angle of reflecting surface was in the interval of

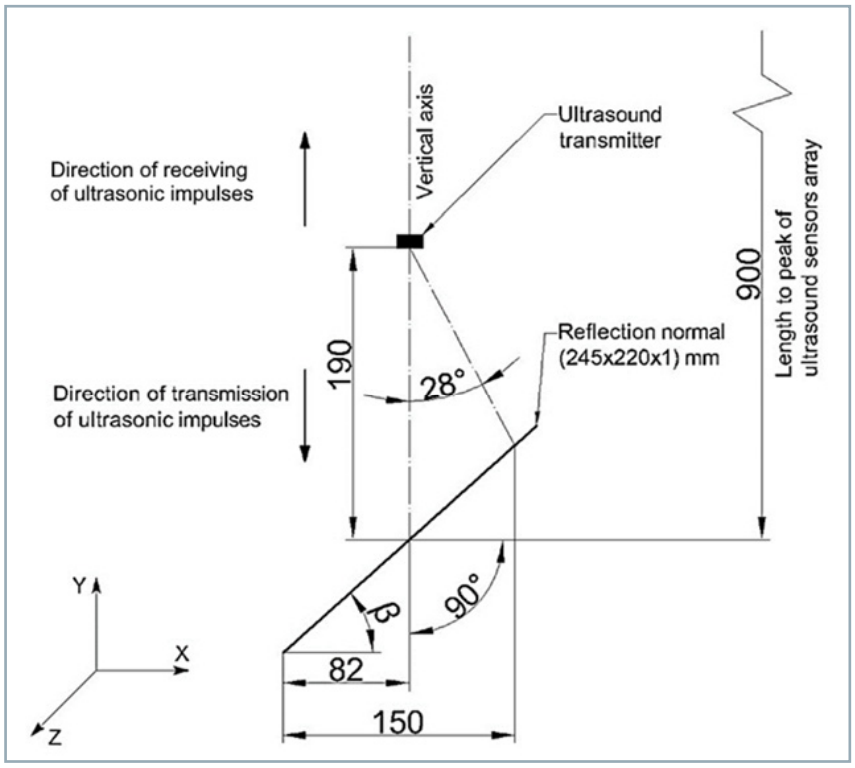



**Fig. 2** Measurement conditions at ultrasonic transmitter side

0–30° with respect to the critical band of electrically significant attenuation of the directional characteristic of ultrasonic transmitter.

$$h \leq \frac{\Phi dx}{2tg\frac{\varphi}{2}} \quad (7)$$

where: $h$ – distance between the ultrasonic transmitter and the reflecting surface (m); $\Phi dx$ – the critical (lowest) dimension of the reflection vector (m); $\varphi$ – confidence angle of the ultrasonic sensor (°)

The ultrasonic transducers were distributed parabolically in an arrangement with a fictive radius of 784.5 mm, chord length of 1086 mm, and angular vectors referenced to the peak distance of the parabolic disposition from reflection surface of 900 mm. The arc length of ultrasonic sensor distribution construction was 1200 mm.

A graphical representation of the angular vectors at the side of the ultrasonic sensors is shown in Fig. 3. The angular vectors are related to the distance between reflected surface and top of the ultrasonic sensor distribution, which was set to 900 mm. The measuring system was installed under laboratory conditions at an air temperature of 21 °C. When measuring the reflection of ultrasound signal from a straight surface, the tilt angle was $\beta = 0°$. The longitudinal axis of ultrasonic sensor distribution (Fig. 3) was parallel to the *X*-axis (Fig. 2). The ultrasound signal reflection from tilted surface was measured when the longitudinal axis of the ultrasonic sensor distribution (Fig. 3) was parallel to the vector of tilt angle $\beta$ of tilted surface (*X*-axis in Fig. 2). In case of parallel measurement, the vertical axis of parabolic distribution of the ultrasonic sensors (Fig. 3) was in line with the vertical axis of ultrasound impulse transmission (Fig. 2). In case of perpendicular measurement, the vertical axis of parabolic distribution of the ultrasonic sensors (Fig. 3) was also in line with the vertical axis of ultrasound impulse transmission (Fig. 2).

Subsequently, the measurement of ultrasound signal reflections was performed at the perpendicular plane of longitudinal axis of the ultrasonic transducer distribution (Fig. 3) to the translation of angular vector $\beta$ on the *X*-axis (Fig. 2). The tilt angle $\beta$ of tilted surface was set to: $\beta = 0°$; 25° and 30°.

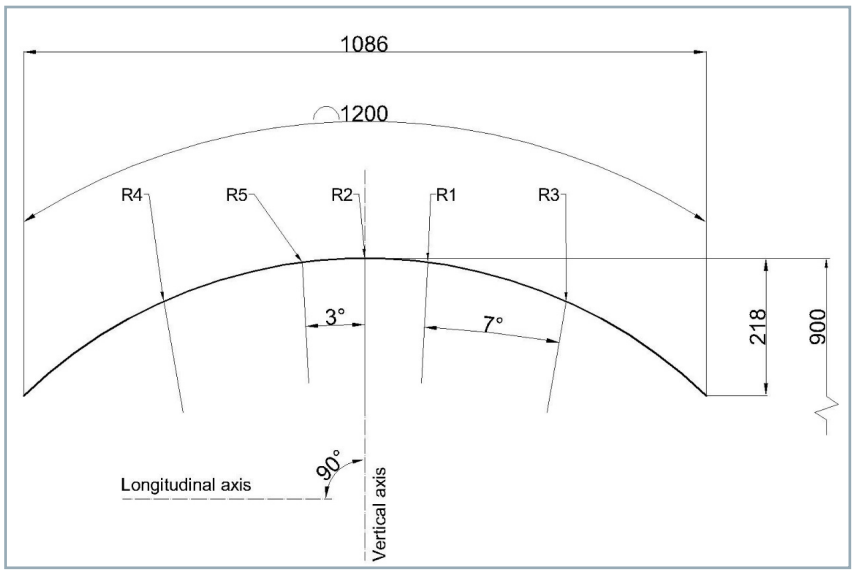



**Fig. 3** Angular vectors related to distance with value 900 mm

## Statistical processing of results

The processing of measured data was performed in the MATLAB R2015b environment. A system identification by iteration method in complex variables as a continuous case of impulse response characteristic was used. The results were subjected to statistical analysis of one-factor analysis of variance. Statistically significant differences were determined by Dunnett's and Tukey's Post-Hoc tests at a significance $\alpha = 0.05$. A statistically significant difference (mark: * in Dunnett's test) was taken into consideration when the critical probability *p*-value of the Post-Hoc test statistics satisfied the condition: *p*

≤0.05. To satisfy the first derivative according to Euler, the differences in amplitudes with value at least of -3 dB were considered significant. Statistical analysis was performed in Statistica 10. Results are expressed as the arithmetic mean ±standard error of the arithmetic mean. The normality of measured data was verified by Shapiro-Wilk test at a significance level of 0.05. The front time determination of transient functions was determined by a functional interval of 10.0–50.0% of the function global maximum in positive derivative. The linearity of relationships was tested by Pearson's correlation coefficient r.

## Results and discussion

### Measurement of reflected ultrasound signal from a straight surface

For the distance from the ultrasonic transmitter to reflection surface, the conic integral for the directional angle of the ultrasonic transmitter ±27.5° was followed. For the statistical significance of the ultrasound impulse amplitude alone, it was concluded that a significance level of 10.0% was satisfactory at the $\alpha = 0.05$ significance level. The modelling of impulse functions was followed by the closeness criterion of the given significance. For the number of poles and zeros, a criterion was heuristically defined: the number of poles corresponds to the minimum number of functionally significant inflection points, and the number of zeros corresponds to at least two crossings of the function with the time axis in the plane of real variable. Quantification of the identified signal in the ultrasonic sensor was performed by calculating the envelope using the Hilbert transform according to Eq. 6. The impulse equation has universal form (Eq. 8).

$$G(s) = \frac{b_0 + b_1 s + \ldots}{a_0 + a_1 s + a_2 s^2 + a_3 s^3 + a_4 s^4 + a_5 s^5 + \ldots} \quad (8)$$

The steady-state value in time was obtained by the complex integral (3). The mean values of amplitudes ±standard error of arithmetic means is shown in Fig. 4.

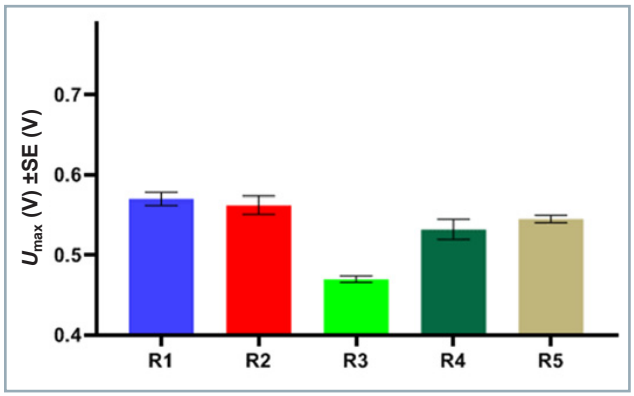



**Fig. 4** Statistical evaluation of mean amplitudes in ultrasonic sensors

All sensors showed good conformity to the normal probability distribution, except sensor R4. Therefore, Kruskal-Wallis test for the statistical significance of difference was used at the unchanged significance level. Modelled impulse functions were compared in terms of the coefficient of determination $R^2$ with the corresponding ultrasonic sensor. The statistical insignificance of difference between the mean amplitude at the R1 sensor versus the middle R2 sensor indicates minimal geometric deviations at the peak vertical. Therefore, let us locally consider the peak sensing point to be the centre of the guide between the sensors R2 and R1. The constant coefficients of individual transfer functions according to Eq. 8 together with the steady-state values according to Eq. 3 are given in Table 2.

The marking of individual impulse functions with an ordinal number (Fig. 5) corresponds to the numbering order of the given ultrasonic sensor. The variability of amplitudes in non-tilted case at 0° angle (sensor R2) is described by a coefficient of variation with a value of 2.049%, which is similar to the relative error of the optical sensor measurement, in which Hrubý et al. (2022) reached a relative error of 1.903% from the true distance in the range of measurements up to 2000 mm.

**Table 2** Constant coefficients of impulse functions with quantification markers

| Sensor | Constant numerator coefficients / Constant denominator coefficients | $R^2$ (%) | $y(\infty)$ | Front time (s) |
|---|---|---|---|---|
| R1 | $1.906 \times 10^{18}$; -6.723 × $10^{14}$; $1.410 \times 10^{11}$ / $1.590 \times 10^{17}$; $2.231 \times 10^{14}$; $1.037 \times 10^{11}$; $3.840 \times 10^{7}$; 5094; 1 | 85.27 | 11.99 | $4.155 \times 10^{-4}$ |
| R2 | $1.483 \times 10^{18}$; -5.233 × $10^{14}$; $1.286 \times 10^{11}$ / $1.283 \times 10^{17}$; $1.886 \times 10^{14}$; $8.529 \times 10^{10}$; $3.509 \times 10^{7}$; 4374; 1 | 81.24 | 11.56 | $4.168 \times 10^{-4}$ |
| R3 | $5.974 \times 10^{17}$; -2.507 × $10^{14}$; $6.224 \times 10^{10}$ / $5.096 \times 10^{16}$; $1.076 \times 10^{14}$; $4.452 \times 10^{10}$; $2.641 \times 10^{7}$; 2878; 1 | 78.98 | 11.72 | $5.233 \times 10^{-4}$ |
| R4 | $1.738 \times 10^{18}$; -6.235 × $10^{14}$; $1.195 \times 10^{11}$ / $1.531 \times 10^{17}$; $2.238 \times 10^{14}$; $1.068 \times 10^{11}$; $3.811 \times 10^{7}$; 5466; 1 | 87.77 | 11.36 | $4.340 \times 10^{-4}$ |
| R5 | $2.628 \times 10^{18}$; -7.839 × $10^{14}$; $1.561 \times 10^{11}$ / $2.302 \times 10^{17}$; $3.063 \times 10^{14}$; $1.326 \times 10^{11}$; $4.493 \times 10^{7}$; 5703; 1 | 90.37 | 11.41 | $4.074 \times 10^{-4}$ |

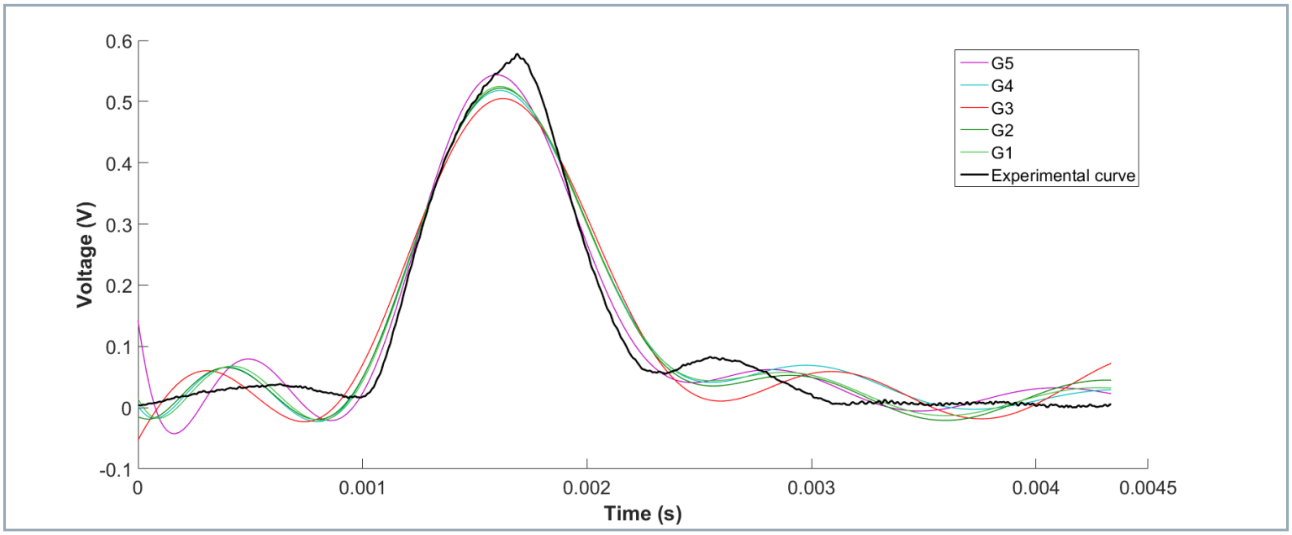



**Fig. 5** Simulation of impulse functions in ultrasonic sensors at 0° tilt angle (sensor R2 is considered an experimental curve)

### Measurement of reflected ultrasound signal from a tilted surface

For the measurement of ultrasound signal reflections from a tilted surface, the distances between the ultrasonic transmitter and reflecting surface or the reflecting surface and ultrasonic sensor distribution were the same as for the measurement of ultrasound signal reflections from a straight surface.

### Measurement of reflections from an inclined plane with a parallel longitudinal axis of the sensor distribution

The significance analysis of amplitude differences in respect to the peak sensor (R2 sensor) showed statistically significant differences in all cases (Fig. 6). The statistical processing of signal amplitudes in each sensor is shown in Fig. 6.

The neighbourhood of angular differences in signal amplitude was verified by Tukey's test; the statistical non-significance of the difference was demonstrated in case of the sensors R1 and R3, interpreting this result as an amplitude dominance of the sensors R2, R4 and R5. The direction of variation of reflection surface tilt angle is directly proportional to the functional dominance in signal amplitude in the ultrasonic sensors. The maximum variability in case of reflection from a straight surface vs. a tilted surface did not exceed the coefficient of variation $V_k \leq 2.50\%$. The criterion of -3 dB in attenuation in relation to the global maximum (sensor R4) was met by all sensors. Neither of the sensors satisfied the 10.00% attenuation criterion at the significance level $\alpha = 0.05$. The modelling of impulse functions of individual sensors along with the quantification markers according to Eq. 8 and steady state with respect to Eq. 3 is presented in Table 3. The amplitude aspect of the steady-state $y(\infty)$ values in decreasing order shows the signs of the hypothesis of signal-dominated sensors and thus of a directional tilt. However, the condition of neighbourhood of an angle is broken, where a sequence can be observed (R4, R2, R1, R5 and R3). The sensors R1 and R3 have the highest values of the front time of transient characteristics. From the point of view of reflection surface tilt angle, these are the non-dominant sensors in the signal amplitude.

Considering the graphical preparation (Fig. 6), it can be concluded that the ultrasound signal amplitudes are directly proportional to the angle of inclination variation of reflecting surface and inversely proportional to the temporal time transients found in the impulse function on the scalar quantifier of steady state.

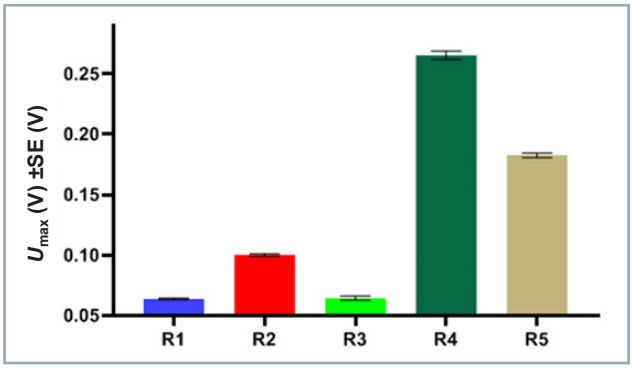



**Fig. 6** Statistical processing of average signal amplitudes in each ultrasonic sensor

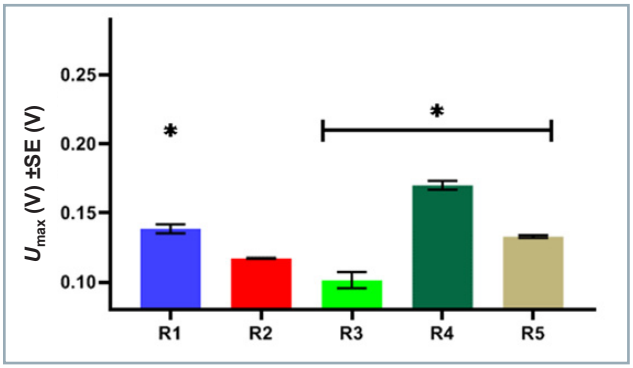



**Fig. 7** Statistical processing of average signal amplitudes in each ultrasonic sensor

**Table 3** Constant coefficients of impulse functions with the quantification markers

| Sensor | Constant numerator coefficients<br>Constant denominator coefficients | $R^2$ (%) | $y(\infty)$ | Front time (s) |
|---|---|---|---|---|
| R1 | $1.442 \times 10^{18}$; $-1.017 \times 10^{14}$; $6.074 \times 10^{10}$<br>$6.477 \times 10^{17}$; $9.830 \times 10^{14}$; $5.908 \times 10^{11}$; $8.365 \times 10^{7}$; $1.031 \times 10^{4}$; 1 | 58.26 | 2.257 | $9.225 \times 10^{-4}$ |
| R2 | $1.253 \times 10^{18}$; $-1.379 \times 10^{14}$; $5.523 \times 10^{10}$<br>$4.817 \times 10^{17}$; $6.033 \times 10^{14}$; $2.459 \times 10^{11}$; $7.203 \times 10^{7}$; $1.020 \times 10^{4}$; 1 | 92.07 | 2.600 | $6.752 \times 10^{-4}$ |
| R3 | $2.508 \times 10^{18}$; $-1.672 \times 10^{14}$; $1.103 \times 10^{11}$<br>$1.453 \times 10^{18}$; $1.887 \times 10^{15}$; $5.575 \times 10^{11}$; $1.050 \times 10^{8}$; $1.186 \times 10^{4}$; 1 | 80.21 | 1.723 | $7.827 \times 10^{-4}$ |
| R4 | $-1.251 \times 10^{19}$; $2.233 \times 10^{15}$; $-3.512 \times 10^{11}$<br>$2.959 \times 10^{18}$; $1.928 \times 10^{15}$; $1.102 \times 10^{12}$; $1.404 \times 10^{8}$; $3.234 \times 10^{4}$; 1 | 92.00 | 3.949 | $3.206 \times 10^{-4}$ |
| R5 | $-2.105 \times 10^{19}$; $9.976 \times 10^{14}$; $-1.103 \times 10^{11}$<br>$1.002 \times 10^{19}$; $3.262 \times 10^{15}$; $2.377 \times 10^{12}$; $1.449 \times 10^{8}$; $3.935 \times 10^{4}$; 1 | 81.10 | 1.772 | $2.135 \times 10^{-4}$ |

### Measurement of reflections from an inclined plane with a perpendicular longitudinal axis of the sensor distribution

The distances remained the same with respect to the previous experiment. The normal probability distribution of signal amplitudes was obtained for all sensors by Shapiro--Wilk test.

Statistically significant differences were found by Dunnett's test (Fig. 7) in relation to the peak sensor (sensor R2) for all other sensors. The non-significance of difference in signal amplitudes in neighboured sensors was indicated by Tukey's test in case of the sensor R1 vs. R5 pair. The results of impulse functions modelling with respect to Eq. 8 and steady state with respect to Eq. 3 are presented in Table 4 along with the quantification markers.

The highest steady-state values of impulse functions (Table 4) are directly proportional to the front times of transient characteristics. When investigating the dependence of front time on the steady-state value of transient characteristic, Pearson's coefficient showed a value of $r$ = 0.184 in case of reflection from an un-tilted surface, indicating a weak linear dependence. In case of a tilted surface and parallelism of the longitudinal axis of the ultrasonic transducer distribution, Pearson's correlation coefficient showed a value of $r$ = -0.308, indicating a poor non-linear dependence. In case of a tilted plane and perpendicular of the longitudinal axis of transducer distribution, Pearson's correlation coefficient reached a value of $r$ = 0.487, indicating a medium linear dependence. To verify the dependence nature of front time on the steady-state value, there was performed an analysis when the reflecting surface tilt angle varied to a value of 25°. In case of parallel longitudinal axis of ultrasonic sensors distribution, Pearson's coefficient resulted in a value of $r$ = -0.990, indicating an extraordinarily strong non-linear dependence between the steady-state value of impulse function and front time value. The number of poles and zeros of impulse functions was the same as in the previous examples, i.e., 5 poles and 2 zeros. In case of the parallel longitudinal axis of ultrasonic sensors distribution, the coefficient of determination was in the range of 78.52–92.10%. The coefficient of determination for the perpendicular longitudinal axis of the ultrasonic sensors was in the range of 86.54–91.96%. For all the cases observed, the measurement uncertainty for the position vector of transmission and the acquisition of ultrasound impulses at a distance of 1090 mm was 0.858 mm at

**Table 4** Constant coefficients of impulse functions with the quantification markers

| Sensor | Constant numerator coefficients<br>Constant denominator coefficients | $R^2$ (%) | $y(\infty)$ | Front time (s) |
|---|---|---|---|---|
| R1 | $1.975 \times 10^{18}$; $-3.308 \times 10^{14}$; $8.968 \times 10^{10}$<br>$5.252 \times 10^{17}$; $8.976 \times 10^{14}$; $2.360 \times 10^{11}$; $7.310 \times 10^{7}$; 6022; 1 | 81.99 | 3.760 | $6.174 \times 10^{-4}$ |
| R2 | $1.599 \times 10^{14}$; $-2.770 \times 10^{10}$; $6.730 \times 10^{6}$<br>$4.808 \times 10^{13}$; $6.049 \times 10^{10}$; $3.586 \times 10^{7}$; 2445; 1 | 71.54 | 3.457 | $6.351 \times 10^{-4}$ |
| R3 | $1.582 \times 10^{14}$; $-6.252 \times 10^{9}$; $5.045 \times 10^{6}$<br>$7.014 \times 10^{13}$; $6.036 \times 10^{10}$; $4.565 \times 10^{7}$; 1709; 1 | 73.44 | 2.571 | $6.903 \times 10^{-4}$ |
| R4 | $1.581 \times 10^{18}$; $-3.173 \times 10^{14}$; $3.600 \times 10^{10}$<br>$3.085 \times 10^{17}$; $5.735 \times 10^{14}$; $1.757 \times 10^{11}$; $6.298 \times 10^{7}$; 4403; 1 | 89.10 | 5.122 | $6.185 \times 10^{-4}$ |
| R5 | $1.683 \times 10^{18}$; $-2.129 \times 10^{14}$; $3.540 \times 10^{10}$<br>$3.227 \times 10^{17}$; $7.762 \times 10^{14}$; $1.776 \times 10^{11}$; $6.543 \times 10^{7}$; 4497; 1 | 85.48 | 5.211 | $11.000 \times 10^{-4}$ |

a sampling rate of 200 kHz (Qiu et al., 2022). The confidence interval of transfer functions of the impulse characteristics in non-tilted and tilted cases were at 4.78% by applying the functional dependency of dynamic impulse functions by the linearity of Laplace transform in the distance measurement error interpretation reached by Moreira et al. (2020). It can be concluded that the uncertainty of the impulse functions of tilted surface is comparable to the correction coefficient variability modelling the amplitude of the ultrasound signal according to Martínez et al. (2003), with a coefficient of variation equal to a maximum value of 14.085%.

## Conclusion

The application of measuring methods for position measurement is a constantly developing topic of applied research. The paper presented observes the results of modelling the impulse response functions of ultrasonic transducers. The non-linear dependence of time parameter in the front time domain of transient characteristic of impulse function, correlated with the scalar of the complex integral to the function steady state, directly determines the state that is reached when the slope angular vector of reflecting surface is parallel to the angular vectors of ultrasonic sensor distribution. The ultrasound impulse amplitude was a critical criterion along with angular adjacency in terms of the geometry of ultrasonic transducer deployment. By frequency filtering of the signal of ultrasonic sensors, a decrease in the order of transfer function of the ultrasonic sensor is expected.

## Acknowledgments

These publications have been produced with the support of the Operational Programme Research and Innovation for the project: Support of research activities at SPU Nitra in the field of energy, 313011X029, co-financed by the European Regional Development Fund.

The article was supported by the project of Ministry of Education, Science, Research and Sport of the Slovak republic: KEGA 006SPU-4/2021 Implementation of technology of Industry 4.0 in education process in study program "Control Systems in Production Engineering".

## References

FIKAR, M. – MIKLEŠ, J. 1999. Identification of Systems. Bratislava : STU, 114 pp. ISBN 8022711772 (In Slovak: Identifikácia systémov)

HRUBÝ, D. – VACHO, L. – KUBÍK, Ľ. – TÓTH, L. – BALÁŽI, J. – KÓSA, P. – KIŠEV, M. 2022. Characteristics of distance errors of infrared sensor relation to colour surfaces. In Acta Technologica Agriculturae, vol. 25, no. 1, pp. 40–46. DOI: https://doi.org/10.2478/ata-2022-0007

ISHIKARA, M. – SHIINA, M. – SUZUKI, S. 2009. Evaluation of method of measuring distance between object and walls using ultrasonic sensors. In Journal of Asian Electric Vehicles, vol. 7, no. 1, pp. 1207–1211. DOI: https://doi.org/10.4130/jaev.7.1207

KEYSIGHT. 2021. Keysight U2300A Series USB Multifunction Data Acquisition Devices. Malaysia : Keysight Technologies, 84 pp.

KUC, R. – SIEGEL, M. 1987. Physically based simulation model for acoustic sensor robot navigation. In IEEE Transactions on Pattern Analysis and Machine Intelligence, vol. 9, no. 6, pp. 766–778. DOI: https://doi.org/10.1109/TPAMI.1987.4767983

LENDELOVÁ, J. – CVIKLOVIČ, V. – OLEJÁR, M. – POGRAN, Š. 2017. Animal Position Identification Logging System. Slovak patent no. 288467 (In Slovak: Záznamový systém polohovej identifikácie zvierat)

LIM, J. H. – LEONARD, J. J. 2000. Mobile robot relocation from echolocation constraints. In IEEE Transactions on Pattern Analysis and Machine Intelligence, vol. 22, no. 9, pp. 1035–1041. DOI: https://doi.org/10.1109/34.877524

LU, Z. 2014. Estimating time-of-flight of multi-superimposed ultrasonic echo signal through envelope. In 2014 International Conference on Computational Intelligence and Communication Networks. Bhopal : IEEE, pp. 300–303. DOI: https://doi.org/10.1109/CICN.2014.74

MARTÍNEZ, M. – BENET, G. – BLANES, F. – PÉREZ, P. – SIMÓ, J. E. 2003. Using the amplitude of ultrasonic echoes to classify detected objects in a scene. In ICAR 2003 : Proceedings of the 11th International Conference on Advanced Robotics. Coimbra : University of Coimbra. ISBN 9789729688997

MARTÍNEZ, M. – BENET, G. – BLANES, F. – SIMÓ, J. E. – PÉREZ, P. – POZA, J. L. 2004. Wall/corner classification. A new ultrasonic amplitude-based approach. In IFAC Proceedings Volumes, vol. 37, no. 8, pp. 663–668. DOI: https://doi.org/10.1016/S1474-6670(17)32054-2

MICROCHIP TECHNOLOGY. 2014. TC4426/TC4427/TC4428. Datasheet. 28 pp. Available at: https://ww1.microchip.com/downloads/en/DeviceDoc/20001422G.pdf

MOREIRA, T. F. M. – LIMA, J. – COSTA, P. – CUNHA, M. 2020. Low Cost Binaural System Based on the Echolocation. In Proceedings of the 16th International Conference on Informatics in Control, Automation and Robotics – Volume 1: ICINCO. Setúbal : SciTePress, pp. 818–825. ISBN 9783030361495

PARE, A. – ZHANG, S. – LEI, Z. 2020. Multipath interference suppression in time-of-flight sensors by exploiting the amplitude envelope of the transmission signal. In IEEE Access, vol. 8, pp. 167527–167536. DOI: https://doi.org/10.1109/ACCESS.2020.3023083

PRO-WAWE. 2005. 400ST/R160. Air Ultrasonic Ceramic Transducers. Available at: http://www.prowave.com.tw/index.htm

QIU, Z. – LU, Y. – QIU, Z. 2022. Review of ultrasonic ranging methods and their current challenges. In Micromachines, vol. 13, no. 4, article no. 520. DOI: https://doi.org/10.3390/mi13040520

RABADAN, J. – GUERRA, V. – RODRÍGUEZ, R. – RUFO, J. – LUNA-RIVERA, M. – PEREZ-JIMENEZ, R. 2017. Hybrid visible light and ultrasound-based sensor for distance estimation. In Sensors, vol. 17, no. 2, article no. 330. DOI: https://doi.org/10.3390/s17020330

SHIN, S. – KIM, M.-H. – CHOI, S. B. 2019. Ultrasonic distance measurement method with crosstalk rejection at high measurement rate. In IEEE Transactions on Instrumentation and Measurement, vol. 68, no. 4, pp. 972–979. DOI: https://doi.org/10.1109/TIM.2018.2863999

SMITH, S. W. 1999. The Scientist and Engineer's Guide to Digital Signal Processing. San Diego : California Technical Publishing, 650 pp. ISBN 0966017668

UREÑA, J. – MAZO, M. – GARCÍA, J. J. – HERNÁNDEZ, Á. – BUENO, E. 1999. Classification of reflectors with an ultrasonic sensor for mobile robot applications. In Robotics and Autonomous Systems, vol. 29, no. 4, pp. 269–279. DOI: https://doi.org/10.1016/S0921-8890(99)00059-7

WEBSTER, J. G. – EREN, H. 2014. Measurement, Instrumentation and Sensors Handbook. New York : CRC Press, 1600 pp. ISBN 9781439848883

XU, B. – YU, L. – GIURGIUTIU, V. 2009. Advanced methods for time-of-flight estimation with application to lamb wave structural health monitoring. In Structural Health Monitoring 2009: Proceedings of the Seventh International Workshop on Structural Health Monitoring (2 Volume Set). Lancaster : DEStech Publications, Inc., pp. 1202–1209. ISBN 9781605950075

YATA, T. – OHYA, A. – YUTA, S. 2000. Use of amplitude of echo for environment recognition by mobile robots. In Proceedings. 2000 IEEE/RSJ International Conference on Intelligent Robots and Systems. Takamatsu : IEEE, pp. 1298–1303. ISBN 0-7803-6348-5 DOI: https://doi.org/10.1109/IROS.2000.893198